npj | climate and atmospheric science

Article

Published in partnership with CECCR at King Abdulaziz University

https://doi.org/10.1038/s41612-024-00630-4

Climate warming contributes to the record-shattering 2022 Pakistan rainfall

Yujia You[1,2] ✉, Mingfang Ting[1] & Michela Biasutti[1]

A sequence of torrential rainstorms pounded Pakistan in the summer of 2022, shattering records by massive margins (7 sigma). The severe socioeconomic damages underscore the urgency of identifying its dynamic drivers and relationship with human-induced climate change. Here, we find that the downpours were primarily initiated by the synoptic low-pressure systems, whose intensity and longevity far exceeded their counterparts in history as fueled by a historically-high cross-equatorial moisture transport over the Arabian Sea. The moisture transport has been trending upward since the 1960s and, in 2022, along with the anomalous easterly moisture influx caused by the combination of La Niña and negative Indian Ocean Dipole events, created a corridor of heavy rainfall extending from central India toward southern Pakistan. While it is not yet established whether the observed trend of the cross-equatorial moisture transport has exceeded natural variability, model-based analysis confirms that it is consistent with the fingerprint of anthropogenic climate warming and will raise the likelihood of such rare events substantially in the coming decades.

Pakistan is located at the western edge of the pluvial region of the South Asian summer monsoon. Much of Pakistan's territory receives little rain, especially the southern coasts and the lowland plains of the Indus River[1]. The exception is the northernmost mountains, where moisture in the monsoon flow is lifted over the steep terrain of the Himalayas and condenses to fall as rain or snow[2] (Fig. 1a). Torrential rainfall over Pakistan often produces catastrophic socioeconomic consequences, whether over the northern mountains, where landslides are often triggered, or over the southern low-lying deserts, where water has nowhere to drain and return to river channels. From mid-June until the end of August 2022, a sequence of record-breaking deluges pummeled Pakistan (Fig. 1b), compounding the effect of unprecedented glacial melt[3]. The accumulated rainfall amount exceeded the most notorious flood in 2010 and all instrumental records over the last 50-years[3]. Close to 2000 people perished, over 2.1 million residents were left homeless, more than 75,000 km^2 of Pakistan were inundated, and at least $30 billion (U.S. dollars) in economic damage were suffered[4–7]. The extraordinary magnitude and impact of the 2022 flood make it imperative to identify the physical processes and forcing factors that initiated it.

The causes of the historical floods over Pakistan have been investigated in the literature[8–19]. On the synoptic scale, it is typically the South Asian monsoon low-pressure systems (LPSs) that often trigger deep convection and bring copious rainfall ahead and south of the storm center[8–10]. A large fraction of LPSs originate near the Bay of Bengal and penetrate deeper inland, where they play a crucial role in determining the amount and distribution of the summer rainfall over South Asia[11,12]. It has also been suggested that the upper-level divergence resulting from the extratropical troughs lying aloft northern Pakistan contributed to the extreme rainfall in 1988, 2010, and 2013[13–16]. On the planetary scale, both Pakistan rainfall and its synoptic triggers are influenced by the large-scale South Asian monsoon circulation, which is further regulated by the sea surface temperature (SST) anomalies over the tropical Pacific and Indian Oceans [e.g., El Niño-Southern Oscillation (ENSO), Indian Ocean Dipole (IOD)][17–21].

Nonetheless, the unprecedented intensity of the 2022 event, which shattered the historical record by hundreds of millimeters, puts it beyond what many previous studies considered plausible under the current climate conditions. Tropical SST anomalies (i.e., the La Niña and Indian Ocean Dipole events) and the anomalous upstream blocking over northeastern Europe have been postulated as contributors of the extreme rainfall over Pakistan[22,23]. However, these climate anomalies were not unprecedented. On the other hand, studies reported that climate warming has enhanced Pakistan rainfall intensity by more than 50%[24–27], though the exact mechanisms remain unexplored and the impact of climate warming manifest on longer timescales as gradual changes. The overarching goal of this study is therefore to examine the multiscale triggers of this unprecedented extreme event and to address the question of whether this rare flood was a mere coincidence event resulting from the synergetic interaction of natural fluctuations, or was it instead unlikely to occur without human influence on the climate system.

[1]Lamont-Doherty Earth Observatory, Columbia University, Palisades, NY, USA. [2]Department of Earth and Environmental Sciences, Columbia University, New York, NY, USA. ✉e-mail: yujia@ldeo.columbia.edu

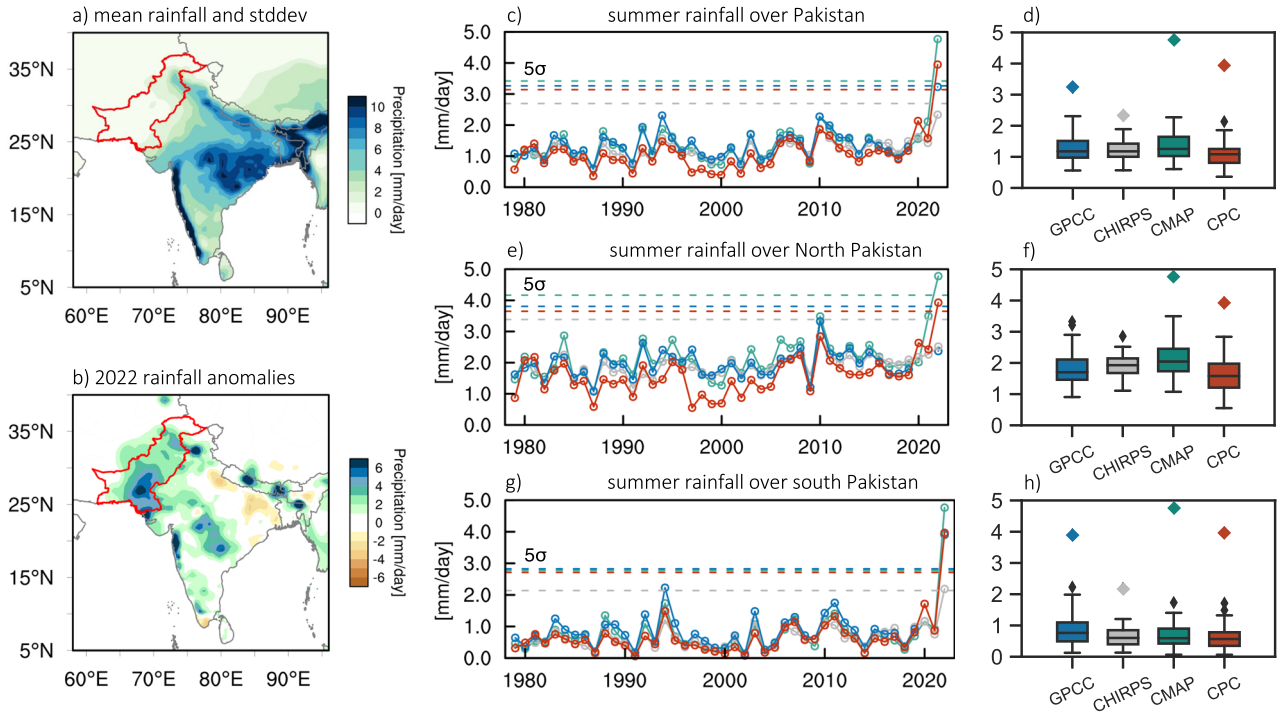

Fig. 1 | Record-shattering Pakistan rainfall in summer 2022. a Climatology of summer (June-September) rainfall (mm/day; shading) and **b** 2022 summer rainfall anomaly (mm/day) based on CPC UNI rainfall dataset. Time series and boxplot of the summer rainfall averaged over **c**, **d** Pakistan, **e**, **f** northern Pakistan (to the north of 30°N), and **g**, **h** southern Pakistan (to the south of 30°N) during 1979–2022. The box extends from the lower to upper quartile, with a line at the median. The whiskers extend from the 5th to the 95th percentile. The black diamonds denote outliers during the period 1979–2021, and the colorful diamonds represent 2022 values. Blue, gray, green, and red colors represent GPCC, CHIRPS, CMAP, and CPC UNI rainfall datasets, respectively. Dashed lines in (**c**, **e**, **g**) denote 5 standard deviations (σ) for the corresponding datasets.

Results

Unprecedented summer rainfall over Pakistan and meteorological triggers

Based on the Climate Prediction Center (CPC) unified gauge-based analysis of daily precipitation, the 2022 summer (June-September) country-wide average precipitation was 3.95 mm/day, exceeding the previous 42-year (1980–2021) average of 1.03 mm/day by 283% and by 7 times its interannual standard deviation (Fig. 1c). The 2022 flood is not only much worse in magnitude but also distinct in its spatial characteristics compared to the notorious flood in 2010, when the rainfall primarily occurred in the wetter northern highlands (Fig. 1e; refs. 13–16). During 2022, the largest rainfall increase was located over the drier southern flat plains (Fig. 1b), where the climatological summer mean rainfall is less than 0.6 mm/day (Fig. 1a, g). The anomalous rainfall was not geographically isolated to Pakistan. Instead, it stretched over a corridor extending northwestward from central India, with the heaviest precipitation concentrated over southern Pakistan (Fig. 1b). While the yearly time series of Pakistan rainfall are highly correlated among the datasets used in the current study, there are some discrepancies in the magnitude of the 2022 rainfall across the different datasets ("Methods" section). However, the 2022 rainfall clearly shows up as the only exceptionally rare event, shattering records by large margins in all datasets, over both southern Pakistan and Pakistan as a whole (Fig. 1d, f, h). This result holds even dating back to 1890 (Supplementary Fig. 1).

From mid-June until the end of August 2022, six unusually intense rainstorms pounded Pakistan (Fig. 2a, blue bars). The 2022 flood was not the result of any singular major rain event, but rather the cumulative effect of multiple episodic heavy deluges. The temporal evolutions of daily rainfall during the six rain pulses are mapped in Supplementary Fig. 2. The most prominent feature, noticeable in all pulses, is the northwestward progression of rainfall hotspots across central India toward Pakistan, which is in agreement with the seasonal rainfall anomalies shown in Fig. 1b. The clear signature of migrating rainfall centers in Supplementary Fig. 2 raises the possibility that the synoptic LPSs, which mostly form near the Bay of Bengal and travel northwestward (Fig. 2b; ref. 26), may have been the culprit of the heavy rainfall events in 2022.

To substantiate this conjecture, we compile the trajectories of South Asian LPSs in the National Aeronautics and Space Administration's Modern-Era Retrospective analysis for Research and Applications, Version 2 (MERRA-2) using an objective feature tracking algorithm (Methods). The green vertical strips in Fig. 2a denote the presence of LPS near Pakistan [i.e., within the Pakistan (PK) box in Fig. 2b]. The trajectories obtained by the tracking algorithm are validated against the manual LPS identification from weather charts (red stripes in Fig. 2a and Supplementary Fig. 3). With the exception of the first rainfall episode in mid-June, all the subsequent five rainfall pulses were triggered by LPSs. The climatological mean distribution of LPS cyclogenesis and cyclolysis locations during the previous 42-year period (1980–2021) are displayed in Fig. 2b, overlapped with the corresponding locations of the 2022 LPSs. Historically, most of the LPSs formed over the Bay of Bengal, propagated northwestward, dissipated over central India, and were incapable of producing much rainfall over Pakistan. In contrast, the majority of the 2022 LPSs traveled beyond the endpoints of the historical LPSs (Fig. 2b, pink dots) and had stronger-than-average cyclone intensity (Fig. 2d, red boxplot). As a consequence, even though the LPS genesis was below-average in 2022 (Fig. 2d, blue boxplot), the LPS activity over Pakistan was record-high (Fig. 2d, green boxplot; Fig. 2c), favoring anomalous heavy rainfall from central India to southern Pakistan (Fig. 2c, blue dots).

Large-scale circulation anomalies and contribution of anthropogenic forcings

The genesis, propagation, and dissipation of synoptic storms are, to a large extent, regulated by the ambient large-scale environment, and specifically by the availability of moisture fueling deep convection and the attendant circulation. How much, then, was the unusually strong 2022 LPS activity due to

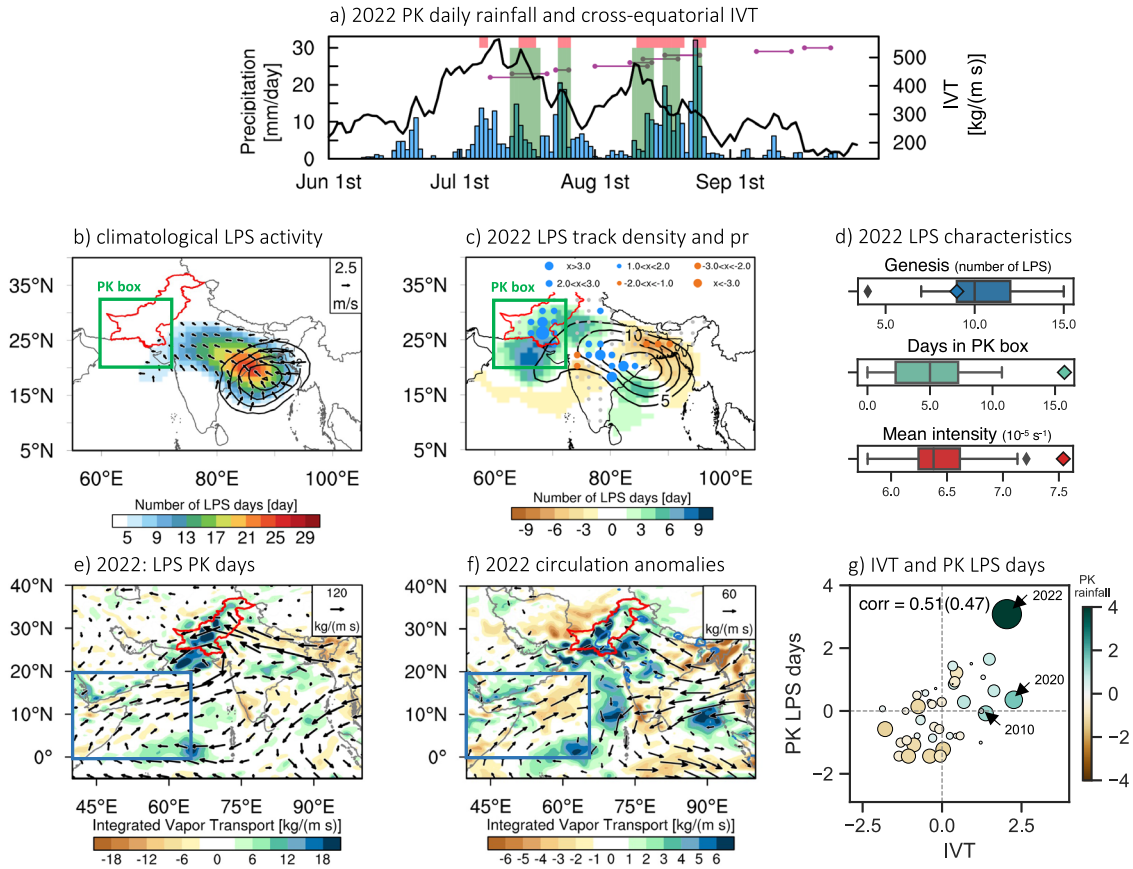

Fig. 2 | Meteorological triggers of 2022 Pakistan rainfall and its control factors. **a** Daily rainfall averaged over Pakistan from June 1st to September 30th, 2022. The purple horizontal lines indicate the lifespan of each individual LPS by objective tracking. The green and red vertical stripes represent the presence of LPS inside Pakistan box (green box in **b**, **c**) based on the objective tracking algorithm and manual tracking method, respectively. The black line denotes the daily cross-equatorial moisture transport, defined as the area-average integrated vapor transport (IVT) over the blue boxed region in **e** (kg m^{-1} s^{-1}). **b** Climatological LPS genesis density (number of LPS per summer; orange contour) and cyclolysis density (number of LPS per summer; blue contour), overlapped with the trajectories of 2022 LPS (green start points, pink ending dots, gray tracks). **c** Anomalies of 2022 LPS track density (number of LPS days; shading) and LPS-related rainfall (mm/day; dots), overlapped with the climatological LPS track density (number of LPS days per summer; contour). **d** LPS genesis number, mean intensity, and days spent in Pakistan box of 2022 LPS (colorful diamonds) as compared to historical LPS (1980–2021; boxplot made in the same manner as Fig. 1d). **e** Composites of anomalous daily moisture fluxes (kg m^{-1} s^{-1}; vector) and its convergence (mm/day; shading) when the 2022 LPS were present in the Pakistan box. **f** 2022 summer mean moisture flux (kg m^{-1} s^{-1}; vector) and its convergence (mm/day; shading) anomalies. **g** Scatter plot of the normalized summer mean cross-equatorial moisture transport (*x* axis) and the normalized number of days when LPS were present in the Pakistan region (*y* axis). Correlations are shown with (0.51) and without (0.47) 2022 values. The size and color of markers indicate the normalized average summer rainfall anomalies over Pakistan.

large-scale circulation anomalies? To explore this question, we determine the large-scale circulation pattern that favored the anomalously strong 2022 LPS activity by compositing those days when the 2022 LPSs were present in the Pakistan box (Fig. 2e). The LPS and intense rainfall were associated with a conveyor belt of water vapor originating from the South Indian Ocean and traveling off the coast of Somalia toward Northwestern India and Pakistan (blue boxed region, Fig. 2e). The potential importance of the landward moisture transport in promoting LPS activity in Pakistan is also evidenced by daily time series of moisture transport, which appears to precondition the presence of LPS over Pakistan and the occurrence of extreme rainfall (Fig. 2a, black solid line) in early July and mid-August. These results suggest that the cross-equatorial transport and the resultant moisture buildup over the subcontinent might supply the fuel needed for LPS-related convection and the energy that sustains the LPS against dissipating forces.

The results in Fig. 2a, e, while strongly suggestive of the role of cross-equatorial moisture transport in sustaining the LPSs from dissipation before they reach Pakistan, may not provide a solid evidence of causality, since the cross-equatorial flow could have been caused by the presence of stronger LPS circulation, which subsequently led to stronger moisture transport over the tropical Indian Ocean (Fig. 2e). To further elucidate the relationship, we compare the moisture transport for the LPS days to the seasonal mean (c.f., Fig. 2e, f). On the seasonal timescale, the transient cyclonic circulation associated with LPS was absent, whereas the above-normal cross-equatorial moisture transport still existed, albeit with a weaker strength (Fig. 2f). Additionally, in accordance with the extraordinary LPS activity, the summer mean cross-equatorial moisture transport was the second strongest in 2022 (Fig. 2g) and its strength is positively correlated with the number of days when the LPS influenced the Pakistan region ($r = 0.51$ and 0.47 with and without 2022, respectively). Note that while the cross-equatorial moisture transport was strong in 2010 and 2022, the moisture flow stagnated over the Arabian Sea and did not ever reach the Indian subcontinent (not shown). The relationship on seasonal-to-interannual timescales indicates a clear causal link: increased cross-equatorial moisture transport over the Arabian Sea can enhance LPS activity over Pakistan. While anomalous moisture import was also noticeable over the Bay of Bengal (Fig. 2f), it did not contribute significantly to the Pakistan LPS activity ($r = -0.26$ without 2022; Supplementary Fig. 4), probably because the background total column water vapor over the Bay of Bengal is already high.

The ultimate cause of the 2022 circulation anomalies can be either natural modes of variability or shifts in the background climate state due to anthropogenic forcings. The yearly time series of the net moisture flux into the Pakistan domain is shown in Fig. 3a, together with its zonal and

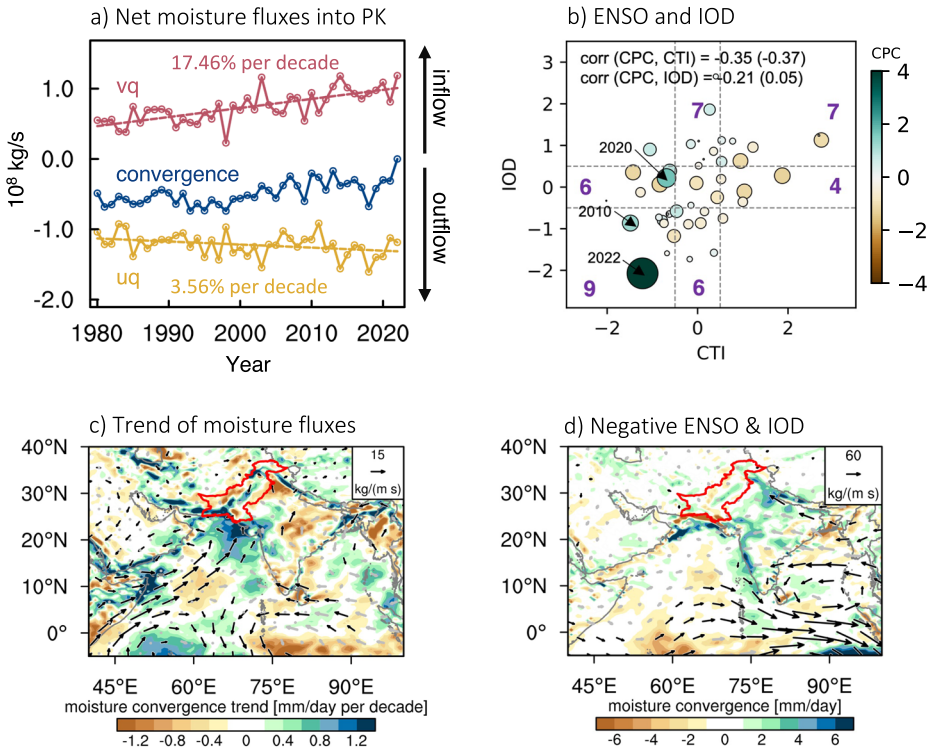

Fig. 3 | Contribution of net moisture fluxes into Pakistan due to anthropogenic forcing and internal variability. a Net moisture inflow into the Pakistan domain (10^8 kg s^{-1}; blue line). Red and yellow lines are for meridional and zonal component, respectively. Significant linear trend fitted to the data as dashed lines. **b** Scatter plot of the normalized summer mean cold tongue index (CTI; 6°S-6°N, 180°−90°W; *x* axis) and Indian Ocean Dipole (IOD) index [SST anomaly difference between the western (10°S-10°N, 50°−70°E) and eastern Indian Ocean (10°S-0°, 90°−108°E); *y* axis] over the period 1980–2022. Extreme ENSO and IOD events defined as exceedances of ± 0.5σ (dashed gray lines) due to the limited sample size. Correlations outside and inside the parentheses are calculated with and without 2022 values, respectively. Purple numbers indicate sample size in each subcategory. **c** Linear trend of moisture fluxes (kg m^{-1} s^{-1} per decade; vector) and its convergence (mm/day per decade; shading) in 1980–2022. **d** Difference of moisture flux anomalies (kg m^{-1} s^{-1}; vector) and its convergence (mm/day; shading) between summers with negative phases of ENSO and IOD and summers with positive phases. The darker vectors in **c**, **d** represent statistical significance at 95% confidence level based on two-sided Student's *t* test. Moisture fluxes and sea surface temperature are taken from MERRA-2 and ERSST v5, respectively.

meridional components (see Methods). Climatologically, the large net outflow of moisture in the zonal direction is partially compensated by the net moisture inflow in the meridional direction. Both components have experienced significant long-term changes. The zonal outflow is trending upward at a rate of 3.56% (-0.44×10^7 kg s^{-1}) per decade, and the meridional inflow is increasing at a rate of 17.46% (1.29×10^7 kg s^{-1}) per decade (Fig. 3a). In 2022, the meridional moisture influx was at a historical high and was favored by the ongoing trend, whereas the zonal outflow was weaker than what the trend would lead us to expect. The combination of a strong inflow and a weak outflow yielded a large anomalous convergence in 2022. The clear monotonic trend in observation is in strong agreement with the projected change made by climate models[28,29], thus highlighting the importance of climate warming in setting the favorable environment for Pakistan flood, though there are certainly contributions from natural modes of variability. The robustness of the upward trend is verified by multiple reanalysis products (Supplementary Fig. 5).

During the summer of 2022, cold SST anomalies were observed over the eastern tropical Pacific and western Indian Ocean with warm SST anomalies in the western tropical Pacific and eastern Indian Ocean (Supplementary Fig. 6). These anomalies are consistent with La Niña conditions, which persisted for a third year, co-occurring with a strong negative IOD (Fig. 3b). La Niña events are associated with stronger-than-normal monsoon circulation and excessive rainfall over the Indian subcontinent[17]. However, the negative IOD events frequently lead to a weakening and southward shift in the monsoon ascending branch, resulting in an unfavorable condition for Pakistan flood[17–21]. In our study period, the Pakistan country-wide average rainfall is negatively correlated with ENSO ($r = -0.37$) but has no statistically significant relationship with IOD ($r = 0.05$ without 2022). Nonetheless, the occurrences of ENSO and IOD events are, to some degree, not independent of each other and their influences on the South Asian monsoon rainfall are coumpounded[19]. To better demonstrate the combined effects of La Niña and negative IOD in our study period, the moisture transport anomalies during summers with negative phases of ENSO and IOD are subtracted from anomalies during summers with positive phases (Fig. 3d). There are similarities between the ENSO-IOD composite and the 2022 anomalies over the Bay of Bengal and the eastern Indian Ocean. In the ENSO-IOD composite, the anomalous easterly moisture flux over central India tend to reduce the moisture outflow over Pakistan (Fig. 3d), hinting that the 2022 Pakistan rainfall could partly arise from intrinsic, natural variability. However, it completely lacks the cross-equatorial moisture transport over the Arabian Sea, which was a strong feature in summer 2022. The absence of the cross-equatorial moisture transport in the ENSO and IOD composite, together with the prominent long-term trend of this moisture transport (Fig. 3c), highlight the contribution of externally-forced climate background shifts.

Increasing likelihood under global warming

To estimate the possible anthropogenic contribution to the cross-equatorial moisture transport, we analyze an ensemble of models participating in the Coupled Model Intercomparison Project, Phase 6 (CMIP6; Methods) and estimate the forced change during the historical period as the multi-model ensemble average. Compared to the notable enhancement in the observed Pakistan summer rainfall (>27% per decade in some regions; Fig. 4a), the externally forced change indicates a moderate but spatially homogeneous increase (4–5% per decade; Fig. 4b). The increase is anchored by an enhanced cross-equatorial moisture transport (Fig. 4c), consistent with

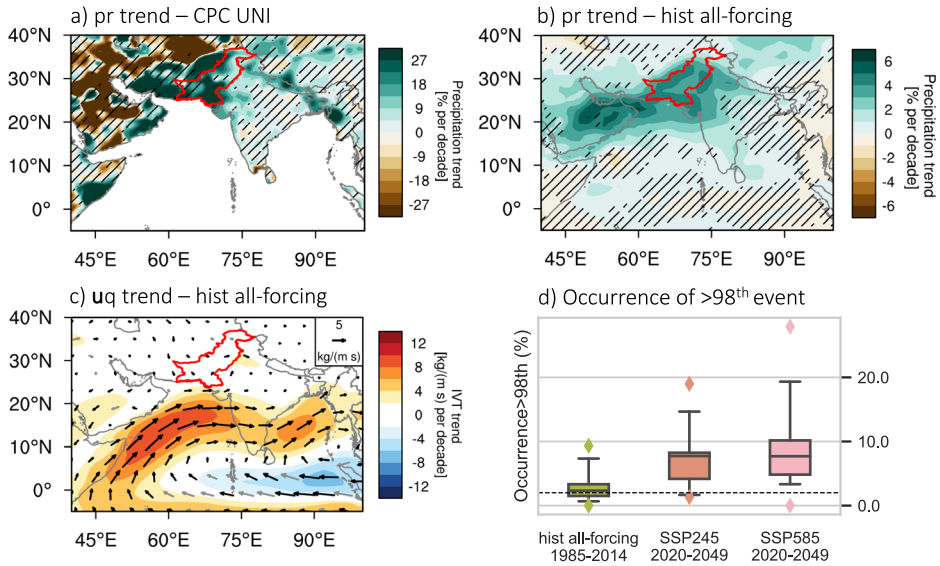

Fig. 4 | Modeled changes in Pakistan rainfall and large-scale monsoon circulation. a, **b** Linear trend of summer rainfall (% per decade; shading) in (**a**) CPC UNI during 1980–2022 and (**b**) historical experiment of CMIP6 models during 1980–2014. **c** Linear trend of summer mean moisture fluxes and its magnitude (kg m^{-1} s^{-1} per decade; shading) in CMIP6 historical all-forcing experiment. **d** Occurrence of Pakistan extreme rainfall (>98th percentile of summer mean Pakistan rainfall in the reference period 1951–1980) in models with ensemble size no less than 5 (bolded models in Supplementary Table 2). The box extends from the lower to upper quartile, with a line at the median. The whiskers extend from the 5th to the 95th percentile. The diamonds denote outliers. Green boxplot for historical experiment during 1985–2014. Orange and pink boxplots for SSP2–4.5 and SSP5–8.5 experiments during 2020–2049. Dashed line represents 2% occurrence. Hatching in (**a**) denotes regions where the observed trends are not significant at 95% confidence level and (**b**) regions where the model ensemble mean trend lacks sufficient model agreements (defined as smaller than 75% models having the same trend sign).

observations (Fig. 3c). Additionally, the forced response is, to a large extent, the consequence of increasing greenhouse gases (GHG), as single-forcing simulation with a subset of the CMIP6 models confirms that GHG alone is sufficient to produce a wetting trend and an increased cross-equatorial moisture transport (Supplementary Fig. 7).

To quantify the impacts of anthropogenic forcings on the occurrence probability of heavy rainfall over Pakistan across models, we calculate the probability of summer seasonal mean Pakistan heavy rainfall (i.e., exceedances of the 98th percentile of summer rainfall over the base period 1951~1980) in each ensemble member for two subsequent 30-year periods, i.e., 1985–2014 and 2020–2049 (Fig. 4d). The 98th percentile is chosen because CMIP6 models are unable to simulate events that have comparable intensity as the 2022 event (i.e., 4–7σ) and such an extreme event rarely occurs in the real world (one event in observational record since the 1980s). In simulations forced with the historical anthropogenic forcings, there is virtually no change in the occurrence of extreme rainfall during the recent past (0–9.3%). Nonetheless, even under a moderate emission scenario (SSP2–4.5), large majority of the models indicate a significant increase in the occurrence of extreme events in the coming decades. Under a higher emission scenario (SSP5–8.5), some of the models project a more extreme enhancement, although the increment is not statistically distinguishable from that in the SSP2–4.5. The strong inter-model consensus on the wetting trend over Pakistan is noteworthy since the agreement is not due to thermodynamic moistening, but due to the dynamical enhancement of the monsoonal cross-equatorial moisture transport (Supplementary Fig. 8) and more frequent LPS activity (Supplementary Fig. 9c). Despite the inter-model agreement on the sign of change, the magnitude of the wetting is still subject to large uncertainty (e.g., 1.7–19% under SSP2–4.5). Though a complete analysis of the source of this uncertainty is beyond the scope of the present study, we impute it to the models' varying ability to simulate the LPSs, which cannot be well resolved with coarse resolution models (Supplementary Fig. 9d; ref. 30).

How will the modes of internal variability alter rainfall extremes over Pakistan in the coming decades, as the globe continues to warm? Models indicate that the frequency and intensity of La Niña and negative IOD events remain approximately unchanged from the 1951–1980 reference period to the recent past and near future decades (Supplementary Figs. 10a, b); nonetheless, the Pakistan rainfall anomalies during the extreme phases of these two modes show an unequivocal tendency toward greater magnitude as time progresses (Supplementary Fig. 10c), pinpointing the clear predominance of climate change in the future variability of Pakistan rainfall.

Discussion

Our multiscale investigation examines the meteorological triggers and the large-scale circulation drivers that initiated the unprecedented Pakistan rainfall in summer 2022, which broke records by huge margins (283% and 7σ exceedance). Our goal is to understand if such an extreme event merely resulted from the accidental combination of natural modes of fluctuations, or whether its occurrence relied on the additive effect of the anthropogenically-forced warming and internal variability.

We find that the record-breaking rainfall was not caused by a single major rainfall event, but resulted from the cumulative effect of six episodes of heavy rainfall, which were triggered by the synoptic low-pressure systems (LPSs) migrating northwestward through central India into southern Pakistan. In 2022, the LPS survived longer, traveled farther westward, and resided over the dry Pakistan for an extraordinarily long time as compared to most of their historical counterparts. A comparison of observations and climate models indicates that both internal variability and anthropogenic warming were conducive to the excessive Pakistan rainfall in summer 2022. While the internal variability arising from the sea surface temperature anomalies (i.e., La Niña and negative IOD) promoted Pakistan rainfall by reducing the mean eastward moisture outflow, it was the anthropogenically-driven enhancement in the cross-equatorial moisture transport over the Arabian Sea that supplied the fuel needed for LPS-related convection and consequently, enhanced the ability of LPSs to propagate farther westward into Pakistan before being dissipated. Multiple global reanalyses and models confirm that the cross-equatorial moisture transport in summer 2022, although abnormal, is in line with the

unambiguous upward trend since the 1960s due to anthropogenic warming. Continued warming will cause the probability of extreme Pakistan rainfall to increase substantially in the coming decades, even under a moderate emission scenario.

Methods

Observation

The gridded daily rainfall data are obtained from the Climate Prediction Center (CPC) Unified Gauge-Based Analysis of Global Daily Precipitation (CPC-UNI; ref. 31), Climate Prediction Center Merged Analysis of Precipitation (CMAP; ref. 32), the Global Precipitation Climatology Centre (GPCC; ref. 33), and Climate Hazards center InfraRed Precipitation with Station data (CHIRPS; ref. 34). The reanalysis six-hourly and monthly data at 0.5° x 0.625° lat/lon horizontal grid is taken from the Modern-Era Retrospective analysis for Research and Applications, Version 2 (MERRA-2; ref. 35), which spans the period 1980 to present. Compared to other reanalysis products (JRA-55[36], NCEP/NCAR Reanalysis[37], and ERA5[38]), MERRA-2 is chosen for the current study because of the higher degree of consistency between MERRA-2 rainfall and the gauge-based observations (Supplementary Table 1). The observed monthly sea surface temperature data is taken from the the National Oceanic and Atmospheric Administration Extended Reconstruction of Historical Sea Surface Temperature version 5 (ERSST v5)[39].

Model data

Monthly mean data from models participating in the Coupled Model Intercomparison Project phase 6 (CMIP6; ref. 40) is employed. The historical all-forcing experiment, historical single-forcing experiment, and future projections under scenarios based on the shared socioeconomic pathways (SSPs) were considered. The historical all-forcing simulations is forced with observed time-varying changes in atmospheric composition (natural and anthropogenic) and land cover, whereas the single-forcing simulation is driven solely by greenhouse gases. SSP2–4.5 and SSP5–8.5 correspond to an additional radiative forcing of 4.5 W m^{-2} and 8.5 W m^{-2} by the year 2100, respectively. The information of CMIP6 models and the number of ensemble members can be found in Supplementary Table 2.

Objective feature tracking of the South Asian monsoon low-pressure systems

Due to the overall weaker intensity of the South Asian monsoon LPSs as compared to tropical cyclones, tracking LPSs using reanalysis is challenging using automatic tracking algorithms[10,26,41–43]. The objective algorithm we used to create the objective LPS trajectories is built upon on the *TempestExtreme*[44] with 6-hourly MERRA-2 reanalysis.

Our algorithm mimics manual tracking procedure and generally follows the one discussed in refs. 30,45–47 using 850 hPa relative vorticity and sea level pressure fields. To reduce the bias that may be introduced from intra-seasonal and interannual variability, the synoptic fluctuations in sea level pressure are extracted using a 21-day high-pass filter. To reduce noise, the vorticity and sea level pressure fields are spectrally filtered to retain total wavenumber 5–42 and 5–63, respectively. The algorithm proceeds by identifying LPS candidates that have local vorticity maxima exceeding $4 \times 10^{-5}\,s^{-1}$ at each time step. To remove ambiguous candidates that are too weak to be identified as LPS, a closed contour criterion is further applied to ensure closed circulation centers by requiring a 0.2 hPa increase of sea level pressure increase within 5° of the candidate points. Nearby candidates are then stitched on sequential time steps to form trajectories with a maximum translation distance between candidates of 5°. Candidates that do not exhibit behavior consistent with a transiting feature are eliminated. Finally, only cyclones that last at least 2 days and have at least 1 track point within the domain 10°N-35°N, 60°E-95°E are retained. The bash script to obtain our LPS trajectories using *TempestExtremes* can be found in Supplementary Method 1. The parameters of the tracking algorithm were determined and validated to best match the manual tracking results of 2022 LPS provided by the Pakistan Meteorological Department (Extended Data Fig. 2b; ref. 3).

To measure LPS activities, the genesis density, track density, and translation velocity, are calculated. The genesis (track) density is computed by counting the number of LPS genesis (track) points within 500 km of each grid point each summer from June to September. Because the LPS locations are reported at 6-hourly time interval, we further divide the track density by four to convert the unit into number of LPS days. The translation velocity is computed using neighboring track positions. Daily rainfall is considered to be LPS-induced when a LPS is present within 500 km radius of the grid point during a time window of ±1 day. The time window of ±1 day is used to accommodate the potential underestimation due to the rainfall daily resolution, since precipitation from a single storm can occur within a consecutive time window[48,49].

Moisture budget analysis

The column-integrated moisture budget for a steady-state atmosphere can be written in pressure coordinates as

$$P - E = -\frac{1}{gp}\nabla\bullet\int_0^{ps}(uq + vq)\,dp, \tag{1}$$

where P represents precipitation, E is evaporation, g denotes gravitational acceleration, ρ is the water density, q is specific humidity, u is zonal wind, v is meridional wind, p is pressure and p_s is its surface value.

For Pakistan region (20°N-32.5°N, 60°E-72.5°E; green boxed region in Fig. 2b), the net moisture budget can be simplified as:

$$<P - E> = -\frac{1}{gp}\oint\left[\int_0^{ps} uqdp\right]ds - \frac{1}{gp}\oint\left[\int_0^{ps} vqdp\right]ds, \tag{2}$$

where the angle bracket represents areal average and $\oint$ denotes contour integral across the Pakistan box lateral boundaries. The first and second terms on the right-hand side represent the net moisture inflow in zonal and meridional direction, respectively.

Data availability

MERRA-2 data used in this study are available at Modeling and Assimilation Data and Information Services Center (https://disc.gsfc.nasa.gov/datasets?project=MERRA-2). CMIP6 data are openly available in the Earth System Grid Federation portal (https://esgf-node.llnl.gov/projects/cmip6/).

Code availability

TempestExtreme can be downloaded from https://github.com/ClimateGlobalChange/tempestextremes. All figures were produced using Python v.3.6 and NCAR Command Language. The codes used for the analyses are available from the corresponding author.

Received: 25 May 2023; Accepted: 21 March 2024;
Published online: 13 April 2024

References

1. Kureshy, K. U. *Geography of Pakistan* (National Book Service, 1997).
2. Kazi, S. A. Climatic regions of West Pakistan. *Pak. Geogr. Rev.* **6**, 1–22 (1951).
3. *Pakistan Meterological Department, Monsoon progress Highlights (1st July to 05th September 2022)*. Accessed on October 2022. https://www.pmd.gov.pk/cdpc/Monsoon_2022_update/Pakistan_Monsoon_2022_Rainfall_Update.html.
4. *South Asian Voices, The Economic Costs of Pakistan's Floods.* Accessed on October 2022; https://southasianvoices.org/the-economic-costs-of-pakistans-floods/ (16 September 2022).
5. *World Food Programme, WFP expands assistance operations to flood-hit communities in Pakistan—complementing Government*

response. Accessed on October 2022; https://www.wfp.org/news/wfp-expands-assistance-operations-flood-hit-communities-pakistan-complementing-government (11 October 2022).
6. *FloodList (2022, August 27) Pakistan—Almost 1,000 Dead, 33 Million Affected in Worst Floods in a Decade.* Accessed on August 2022; https://floodlist.com/asia/pakistan-floods-update-august-2022
7. *Food and Agriculture Organization of the United Nations (2022, September 29) Heavy monsoon rains and subsequent flooding affected large numbers of people and caused widespread devastation to the agricultural sector*. Accessed on October 2022; https://www.fao.org/3/cc2205en/cc2205en.pdf.
8. Houze, R. A., Rasmussen, K. L., Medina, S., Brodzik, S. R. & Romatschke, U. Anomalous atmospheric events leading to the summer 2010 floods in Pakistan. *Bull. Am. Meteorol. Soc.* **92**, 291–298 (2011).
9. Ullah, K. & Gao, S. Moisture transport over the Arabian Sea associated with summer rainfall over Pakistan in 1994 and 2002. *Adv. Atmos. Sci.* **29**, 501–508 (2012).
10. Hurley, J. V. & Boos, W. R. A global climatology of monsoon low-pressure systems. *Q. J. R. Meteorol. Soc.* **141**, 1049–1064 (2014).
11. Rasmussen, K. L. et al. Multiscale analysis of three consecutive years of anomalous flooding in Pakistan. *Q. J. R. Meteorol. Soc.* **141**, 1259–1276 (2014).
12. Cheema, S. B., Zaman, Q., and & Rasul, G. Persistent heavy downpour in desert areas of Pakistan in South Asian monsoon 2011. *Pak. J. Meteorol.* **9**, 71–84 (2012).
13. Bibi, A., Ullah, K., Yushu, Z., Wang, Z. & Gao, S. Role of westerly jet in torrential rainfall during monsoon over Northern Pakistan. *Earth Space Sci.* **7**, 387–396 (2020).
14. Di Capua, G. et al. Drivers behind the summer 2010 wave train leading to Russian heatwave and Pakistan flooding. *npj Clim. Atmos. Sci.* **4**, 1–14 (2021).
15. Yamada, T. J., Takeuchi, D., Farukh, M. A. & Kitano, Y. Climatological characteristics of heavy rainfall in northern Pakistan and atmospheric blocking over Western Russia. *J. Clim.* **29**, 7743–7754 (2016).
16. Hong, C.-C., Hsu, H.-H., Lin, N.-H. & Chiu, H. Roles of European blocking and tropical-extratropical interaction in the 2010 Pakistan flooding. *Geophys. Res. Lett.* **38**, L13806 (2011).
17. Ashok, K., Guan, Z., Saji, N. H. & Yamagata, T. Individual and combined influences of Enso and the Indian Ocean Dipole on the Indian summer monsoon. *J. Clim.* **17**, 3141–3155 (2004).
18. Ashok, K. & Saji, N. H. On the impacts of ENSO and Indian Ocean Dipole events on sub-regional indian summer monsoon rainfall. *Nat. Hazards* **42**, 273–285 (2007).
19. Ashok, K., Guan, Z. & Yamagata, T. Impact of the Indian Ocean Dipole on the relationship between the Indian monsoon rainfall and Enso. *Geophys. Res. Lett.* **28**, 4499–4502 (2001).
20. Syed, F. & Hannachi, A. Inter-annual variability of moisture transport over the northern Indian Ocean and South Asian summer monsoon. *Clim. Res.* **75**, 23–31 (2018).
21. Syed, F. S. & Kucharski, F. Statistically related coupled modes of South Asian summer monsoon interannual variability in the Tropics. *Atmos. Sci. Lett.* **17**, 183–189 (2015).
22. Chen, G., Ling, J., Lin, Z., Xiao, Z. & Li, C. Role of tropical-extratropical interactions in the unprecedented 2022 extreme rainfall in Pakistan: a historical perspective (2023). *Atmos. Res.* **291**, 106817 (2023).
23. Hong, C.-C. et al. Causes of 2022 Pakistan flooding and its linkage with China and Europe heatwaves. *npj Clim. Atmos. Sci.* **6**, 163 (2023).
24. Treydte, K. S. et al. The twentieth century was the wettest period in northern Pakistan over the past Millennium. *Nature* **440**, 1179–1182 (2006).
25. Li, X., Ting, M., Li, C. & Henderson, N. Mechanisms of asian summer monsoon changes in response to anthropogenic forcing in CMIP5 models*. *J. Clim.* **28**, 4107–4125 (2015).
26. Pfahl, S., O'Gorman, P. A. & Fischer, E. M. Understanding the regional pattern of projected future changes in extreme precipitation. *Nat. Clim. Change* **7**, 423–427 (2017).
27. Otto, F. E. L. et al. Climate Change increased extreme monsoon rainfall, flooding highly vulnerable communities in Pakistan. *Environ. Res. Clim.* **2**, 2025001 (2023).
28. Latif, M., Syed, F. S. & Hannachi, A. Rainfall trends in the South asian summer monsoon and its related large-scale dynamics with focus over Pakistan. *Clim. Dyn.* **48**, 3565–3581 (2016).
29. Latif, M., Hannachi, A. & Syed, F. S. Analysis of rainfall trends over indo-pakistan summer monsoon and related dynamics based on CMIP5 Climate Model Simulations. *Int. J. Climatol.* **38**, 3565–3581 (2017).
30. You, Y. & Ting, M. Improved performance of high-resolution climate models in simulating Asian monsoon rainfall extremes. *Geophys. Res. Lett.* **50**, e2022GL100827 (2023).
31. Xie, P., Chen, M., & W. Shi, CPC unified gauge-based analysis of global daily precipitation. *Preprints, 24th Conf. on Hydrology, Atlanta, GA, Amer. Meteor. Soc*., 2.3A. [Available online at https://ams.confex.com/ams/90annual/webprogram/Paper163676.html] (2010).
32. Xie, P. & Arkin, P. A. Global precipitation: A 17-year monthly analysis based on gauge observations, satellite estimates, and numerical model outputs. *Bull. Am. Meteorol. Soc.* **78**, 2539–2558 (1997).
33. Schneider, U. et al. *GPCC Full Data Reanalysis Version 6.0 at 0.5°: Monthly Land-Surface Precipitation from Rain-Gauges built on GTS-based and Historic Data*. https://doi.org/10.5676/DWD_GPCC/FD_M_V7_050 (2011).
34. Funk, C. et al. The climate hazards infrared precipitation with stations—a new environmental record for monitoring extremes. *Sci. Data* **2**, 150066 (2015).
35. Gelaro, R. et al. The modern-era retrospective analysis for research and applications, version 2 (MERRA-2). *J. Clim.* **30**, 5419–5454 (2017).
36. Kobayashi, S. et al. The JRA-55 reanalysis: general specifications and basic characteristics. *J. Meteorol. Soc. Jpn* **93**, 5–48 (2015).
37. Kalnay, E. et al. The NCEP/NCAR 40-year reanalysis project. *Bull. Am. Meteor. Soc.* **77**, 437–471 (1996).
38. Hersbach, H., et al. ERA5 hourly data on pressure levels from 1940 to present. *Copernicus Climate Change Service (C3S) Climate Data Store (CDS)* (2023).
39. Eyring, V. et al. Overview of the coupled model intercomparison Project Phase 6 (CMIP6) experimental design and organization. *Geosci. Model Dev.* **9**, 1937–1958 (2016).
40. Huang, B. et al. Extended Reconstructed Sea Surface Temperature, version 5 (ERSSTv5): Upgrades, vali- dations, and intercomparisons. *J. Clim.* **30**, 8179–8205 (2017).
41. Praveen, V., Sandeep, S. & Ajayamohan, R. S. On the relationship between mean monsoon precipitation and low pressure systems in Climate model simulations. *J. Clim.* **28**, 5305–5324 (2015).
42. Sandeep, S., Ajayamohan, R. S., Boos, W. R., Sabin, T. P. & Praveen, V. Decline and poleward shift in Indian summer monsoon synoptic activity in a warming climate. *Proc. Natl Acad. Sci. USA* **115**, 2681–2686 (2018).
43. Vishnu, S., Boos, W. R., Ullrich, P. A. & O'Brien, T. A. Assessing historical variability of South Asian monsoon lows and depressions with an optimized tracking algorithm. *J. Geophys. Res. Atmos.* **125**, e2020JD032977 (2020).
44. Ullrich, P. A. & Zarzycki, C. M. TempestExtremes: a framework for scale-insensitive pointwise feature tracking on unstructured grids. *Geosci. Model Dev.* **10**, 1069–1090 (2017).
45. You, Y. & Ting, M. Observed trends in the South Asian monsoon low-pressure systems and rainfall extremes since the late 1970s. *Geophys. Res. Lett.* **48**, e2021GL092378 (2021).

46. You, Y. & Ting, M. Low pressure systems and extreme precipitation in southeast and East Asian Monsoon Regions. *J. Clim.* **34**, 1147–1162 (2021).
47. You, Y., Ting, M. & Camargo, S. J. Heavy rain-producing terrestrial low-pressure systems over East Asian summer monsoon region: Evolution, energetics, and trend. *J. Clim*. https://doi.org/10.1175/jcli-d-20-0667.1. (2021)
48. Knight, D. B. & Davis, R. E. Contribution of tropical cyclones to extreme rainfall events in the southeastern United States. *J. Geophys. Res. Atmos.* **114**, D23102 (2009).
49. Khouakhi, A., Villarini, G. & Vecchi, G. A. Contribution of tropical cyclones to rainfall at the global scale. *J. Clim.* **30**, 359–372 (2017).

Acknowledgements

This research was supported by the National Science Foundation Grant AGS16–07348. Y. You. was supported by National Aeronautics and Space Administration (NASA) under the Future Investigators in NASA Earth and Space Science and Technology (FINESST) program – grant 80NSSC20K1656.

Author contributions

M.T. initiated and supervised the project. Y.Y. analyzed data, generated figures, and wrote the first draft of the manuscript with input from M.T. and M.B. All authors discussed and revised the manuscript.

Competing interests

The authors declare no competing interests.

Additional information

Supplementary information The online version contains supplementary material available at https://doi.org/10.1038/s41612-024-00630-4.

Correspondence and requests for materials should be addressed to Yujia You.